CrossMark

Peptide Scaffold-Based Discovery of Nonpeptide Natural Medicines to Target PI3K p85 SH2 Domain

Chong Xu[1] · Jing Leng[1] · Chuncao Wu[1] · Min Yang[1] · Quan Sun[1] · Dan Song[2]

Abstract Targeting phosphoinositide 3-kinase (PI3K) has been recognized as an attractive strategy for anticancer therapy. The PI3K is a heterodimer composed of a catalytic subunit p110 and a regulatory subunit p85. Here, instead of targeting the catalytic p110 that has been considered previously, we purposed targeting the peptide-recognition domain SH2 of regulatory p85 with natural medicines obtained by using a peptide scaffold-based screening scheme. In the procedure, a core binding motif was extracted from the cocrystallized complex of a cognate phosphopeptide with the domain, which was considered as basic scaffold to perform high-through virtual screening against a structurally diverse, nonredundant library of natural products. A number of hit compounds with high binding potency to the domain and significant conformational similarity with the peptide scaffold were identified; in vitro affinity assay confirmed that five hits have moderate or high affinity for the domain with measured dissociation constants K_d range between 25 and 360 μM, which are comparable to or even better than that of the cognate phosphopeptide SDpYMNMTP and its core motif peptide pYMNM ($K_d = 15$ and 32 μM, respectively). Structural analysis and nonbonded comparison of SH2 interactions with phosphopeptides and potent hit compounds revealed that only negatively charged phosphate and, sometime, sulfate can confer domain-binding capability to small-molecule compounds,

but carboxylate cannot. A similar binding mode of compounds with phosphopeptide is important for the compounds to have high affinity and specificity.

Introduction

Phosphoinositide 3-kinase (PI3K) constitutes a family of intracellular lipid kinases that phosphorylate the 3-OH of the inositol ring of phosphatidylinositols (PtdIns) at the plasma membrane lipids and integrate signals from growth factors, cytokines and other environmental cues, translating them into intracellular signals that regulate multiple signaling pathways. These pathways control many physiological functions and cellular processes, which include cell proliferation, growth, survival, motility and metabolism (Enriquez-Barreto and Morales 2016). Activating alterations in PI3K are found frequently in a variety of cancers, making this class of enzymes a prime drug target for anticancer therapy, and tremendous efforts have been devoted to the development of effective PI3K inhibitors (Fresno Vara et al. 2004; Thorpe et al. 2015).

PI3K can be divided into three classes based on their structures and substrate specificities (Jean and Kiger 2014). The class I PI3K is a heterodimer composed of a 110 kDa catalytic subunit (p110) and a 85 kDa regulatory/adapter subunit (p85). The regulatory p85 subunit contains a Src homology 3 (SH3) domain, a breakpoint-cluster region homology (BH) domain between two proline-rich regions, and two SH2 domains separated by an inter-SH2 (iSH2) region, which tightly binds p85 to

✉ Dan Song
8744695@qq.com

[1] Chongqing Academy of Traditional Chinese Medicine, Chongqing 400021, People's Republic of China

[2] Chongqing Technical Centre for Drug Evaluation and Certification, Chongqing 400014, People's Republic of China

the catalytic subunit (Wymann and Pirola 1998), while the catalytic p110 subunit induces the kinase activity of PI3K in multiple cellular signaling pathways. Although a number of small-molecule inhibitors such as Buparlisib (Geuna et al. 2015) and Pictilisib (Vuylsteke et al. 2016) have been developed or are currently under clinical investigation to target PI3K p110, most of them exhibit low selectivity and significant side effects due to the highly conserved feature of the catalytic subunit across PI3K family (Rodon et al. 2013; Chia et al. 2015). The peptides can also interact with and then regulate the function and activity of PI3K and other biologically interesting proteins in a self-binding manner (Yang et al. 2015, 2016; Bai et al. 2017).

Instead of directly targeting the catalytic p110 we herein proposed a peptide scaffold-based discovery of natural product medicines to target the SH2 domain of PI3K p85. SH2 domain is a sequence-specific binding module present in many signaling molecules, which mediates intracellular protein–protein interactions through the recognition of phosphotyrosine motifs on cellular proteins (Pawson et al. 2001). In recent years, targeting SH2 domain with therapeutic peptides has been recognized as a new and promising approach to disrupt biologically relevant protein–protein interactions that are not always ideally suited to be targeted by classical small molecules (Zhou et al. 2013). However, naturally occurring peptides are often not directly suitable for use as convenient therapeutics because they have intrinsic weaknesses, including poor chemical and physical stability, and a short circulating plasma half-life. Some of these weaknesses have been successfully resolved through the molecular design and engineering of therapeutic peptides (Yu et al. 2016). Even so, the active peptide scaffolds are still good candidates and ideal leads to guide the discovery and optimization of new nonpeptide drugs. For example, Kiran and coworkers have successfully identified a nonpeptide analog of the quorum-sensing inhibitor RNAIII-inhibiting peptide (RIP), which can effectively prevents biofilm formation and RNAIII production in vitro as well as device-associated infections in vivo (Kiran et al. 2008). Here, the cocrystallized structures between the N-terminal SH2 domain of PI3K p85 and its cognate phosphopeptide ligands were then used to perform 3D structure-based virtual screening against a commercially available library of structurally diverse natural products. With the screening we were able to identify a number of potential hit compounds candidating as nonpeptide inhibitors of the SH2 domain. The structural basis and molecular mechanism underlying domain–inhibitor recognition and interaction were also elucidated by using molecular docking calculations.

Materials and Methods

Curation of Compound Library

More than 1100 compounds were extracted from the ZINC database (Irwin and Shoichet 2005); they represent a commercially available library and cover a wide variety of natural products, metabolites, derivatives and analogs. First, the druglikeness and pharmacokinetics of these compound candidates were evaluated by empirical Lipinski's rule of five (Lipinski et al. 2001) and ADMET criteria (Segall et al. 2009), respectively. Second, chemical similarity was analyzed over the compound candidates in a pairwise manner; one of two compounds in a pair with high similarity (Tanimoto coefficient >0.85) (Chen et al. 2015) was deleted to improve chemical diversity. Consequently, totally ~60,000 compounds with diverse structure, good druglikeness, and satisfactory pharmacokinetic profile were selected to define a distinct library for subsequent screening.

Molecular Docking

Water molecules and other hetero-atoms were removed from high-resolution crystal structure of PI3K p85 N-terminal SH2 domain in complex with a CD28-derived phosphopeptide (OctP, SDpYMNMTP) (PDB: 5GJI). Considering that the pYMNM are core binding motif of the phosphopeptide ligand of SH2 domain (see "Domain–Peptide Interaction Analysis and Binding Motif Determination" section), the active site was defined as the SH2 residues that can directly contact the motif in the complex structure. The PDB2PQR program (Dolinsky et al. 2007) was used to assign position-optimized hydrogen atoms, utilizing the additional PROPKA (Bas et al. 2008) strategy to predict protonation states at pH = 7.4. The MGLTools utility was used to assign Gasteiger charges to atoms (Morris et al. 2009). Hydrogen atoms were assigned with REDUCE program (Word et al. 1999). A grid box that encompassed the maximum dimensions of the defined active site on SH2 surface was used. The starting translation and orientation of the ligand and the torsion angles of all rotatable bonds were set to random. The Autogrid grid point spacing was set to 0.2 Å. The Autodock parameter file specified ten Lamarckian genetic algorithm runs, 2,000,000 energy evaluations and a population size of 300. Each docking program was used to automatically dock the ligand back into the active site of SH2 domain.

3D Structure-Based Screening and Evaluation

We wanted to identify compounds that mimic the side chain of phosphotyrosine residue (pY) of SH2-binding peptides and have additional groups occupying the subpockets

nearby the pY-binding site. First, compounds with free phosphate, carboxylate, sulphate or nitrate group attached either to an aromatic or aliphatic ring were selected. These compounds were screened against the phosphotyrosine-binding pocket using a flexible ligand docking program Autodock Vina (Trott and Olson 2010), which led to the selection of the top-ranking 100 compounds (Liao et al. 2015). These compounds, in complex with SH2 domain, were one-by-one energy-minimized using OPLS all-atom force filed (Robertson et al. 2015) to better fit the ligands into the binding pocket in the TINKER molecular modeling package (https://dasher.wustl.edu/tinker/).

A 'good' compound should satisfy two criteria (Fig. 1): (a) binding strength (BS): the BS of compound ligands to domain receptor was rescored by using X-Score (Wang et al. 2002), a consensus scoring strategy designed for accurating estimation of the binding free energies of protein–ligand interaction in combination with a variety of molecular docking methods and re-rank them accordingly. (b) Conformational similarity (CS): the binding mode and structural conformation of compound ligands in bound state should be similar and consistent with that of the cognate binders of SH2 domain. The CS between the docked compounds and the core binding motif 'pYMNM' of SH2-binding peptide OctP was calculated using flexible alignment through the Match algorithm of Screen3D method (Kalászi et al. 2014). Practically match algorithm applies first a marking step of the specific atoms with predefined atom types and pharmacophore rules, which are followed by the calculations of minimum and maximum possible intramolecular distances between every atom–atom pair for the compared molecular entities.

Binding Affinity Analysis

The GST-tagged recombinant protein of human PI3K p85 SH2 domain was expressed as a fusion protein in *Escherichia coli* BL21. Bacteria were lysed by sonication in buffer 150 mM NaCl, 15 mM Na_2HPO_4, 5 mM DTT, pH 7.2. The bacterial lysate was incubated with the GST·Bind Resin for 1 h at 4 °C. The resin was then washed three times and then eluted in buffer 50 mM Tris–HCl, 5 mM DTT, pH 7.5. Two phosphopeptides SDpYMNMTP and pYMNM as control were prepared via *F*moc solid phase peptide synthesis, purified to >95% with high-pressure liquid chromatography, and verified by mass spectroscopy. Fluorescence titration analysis of phosphopeptide/compounds to SH2 domain was performed using a Perkin-Elmer fluorescence spectrometer at an excitation wavelength of 290 nm and an emission wavelength of 350 nm as described previously (Schmidt et al. 2007). Phosphopeptides/compounds from stock solutions were added in small increments to 1.6 ml of PBS, 1 mM DTT containing 0.5 µM GST-SH2 proteins. The intrinsic tryptophan fluorescence in the peptide binding pocket of SH2 domain were perturbed due to binding of phosphopeptide/compound ligands into the pocket, which can be monitored as titration curves and used to derive the equilibrium dissociation constants K_d by nonlinear curve fitting.

Fig. 1 Compound candidate was evaluated by two criteria: BS and CS. The former indicates compound binding strength to SH2 domain, while the letter characterizes the conformational similarity between the binding mode of compound and the core binding motif of SH2-binding peptide OctP
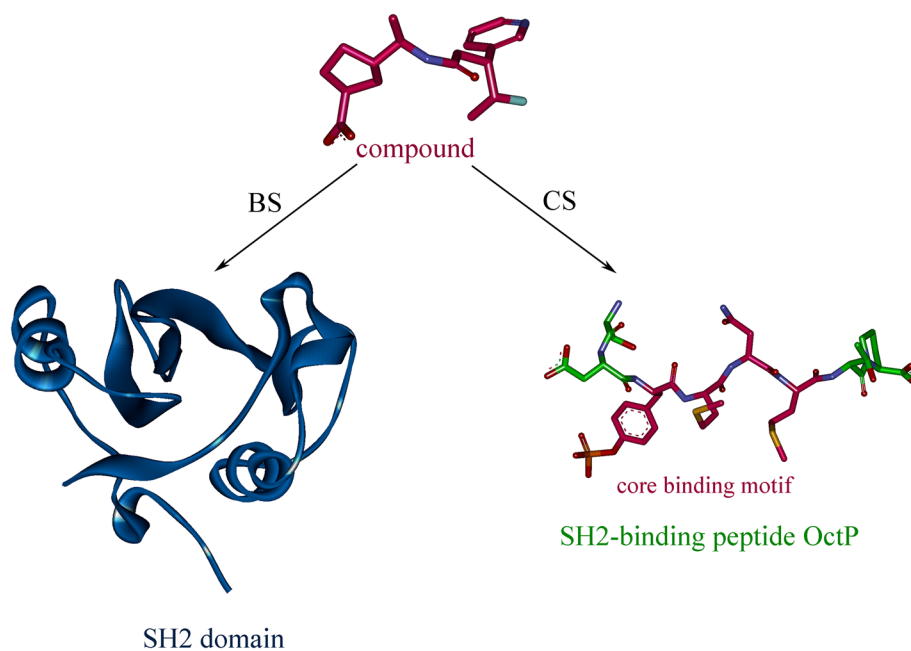
Materials and Methods

Domain–Peptide Interaction Analysis and Binding Motif Determination

The recognition and binding of PI3K to CD28 is an important biological event for CD28-mediated co-stimulatory function in T cell activation. Recently, Inaba et al. have identified a 8-mer phosphopeptide segment (OctP peptide, $S_{-2}D_{-1}pY_0M_{+1}N_{+2}M_{+3}T_{+4}P_{+5}$) on CD28 surface that can be recognized and bound tightly by the N-terminal SH2 domain of PI3K p85 subunit (Inaba et al. 2017). It is known that only the phosphate residue pY is insufficient to support peptide binding against SH2 domain, and additional residues near the pY are required to confer potent affinity and specificity (Gan and Roux 2009). Therefore, a computational truncation analysis was performed on the phosphopeptide to examine its residue contribution. Considering that the pY serves as an anchor in the binding, a series of truncated versions of OctP peptide around pY were generated and their binding potency to the domain were evaluated by CHARMm-based linear interaction energy (LIE) analysis (Gutiérrez-de-Terán and Aqvist 2012) implemented in Discovery Studio (Accelrys, Inc.). The truncation was performed separately at the N- and C-termini of OctP peptide, one residue at a time, until reached at the core pY anchor. Consequently, peptide binding potency change upon the truncation was scored by LIE and shown in Table 1 and Fig. 2. As might be expected, the truncation can reduce the binding capability of OctP peptide to SH2 domain ($\Delta\Delta G > 0$), indicating that all residues in the peptide would contribute to the binding. However, the N-terminus seems to only play a moderate role; deletion of the first two N-terminal residues S_{-2} and D_{-1}, separately resulting in Oct-nS and OctP-nSD, can only induce modest decrease in binding affinity of the native OctP peptide, with ΔScore of 0.2 and 0.8 (<1), respectively. Thus, it is suggested that the two N-terminal residues should contribute very limitedly
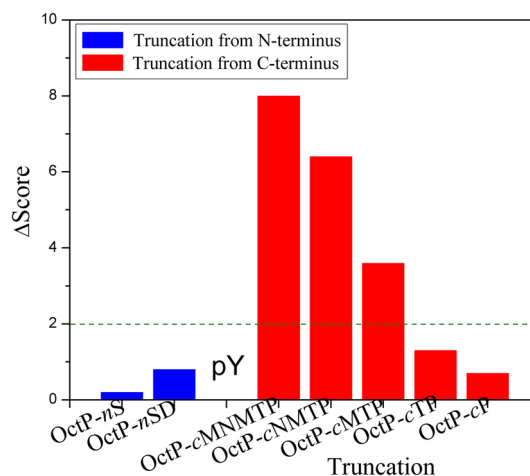

Fig. 2 The change in binding score (ΔSocre) upon peptide truncation. The truncation was performed separately from the N- and C-termini of native OctP peptide, one residue at a time, until reached at the phosphotyrosine anchor pY. nX and cX represent the truncated peptides for which N- and C-terminal residues X were removed relative to the native peptide. (Color figure online)

to OctP binding, which can be removed from the peptide but do not influence its binding capability substantially. Crystal structural analysis of PI3K p85 SH2 domain in complex with OctP peptide revealed that the two residues S_{-2} and D_{-1} N-terminal to pY are out of the peptide-binding pocket of SH2 domain so that they only play a modest role in the domain–peptide binding (Fig. 3). In addition, removal of the first two C-terminal residues T_{+4} and P_{+5} of OctP peptide would result in OctP-cP and OctP-cTP; their binding scores (LIE = 17.0 and 16.4) are very close to that of native OctP peptide (LIE = 17.2) (Table 1). As can be seen in Fig. 3, the peptide primarily uses its pY anchor and central portion to effectively interact with the domain; a number of nonbonded contacts such as hydrophobic forces and hydrogen bonds can be observed at the domain–peptide complex interface, while the C-terminus is weakly packed against the pocket.

Table 1 LIE score of different truncated versions of OctP peptide binding to PI3K p85 SH2 domain

Peptide		Sequence	Score[a]	ΔScore
Native	OctP	SDpYMNMTP	17.2	0
Truncation from N-terminus	OctP-nS	DpYMNMTP	17.0	0.2
	OctP-nSD	pYMNMTP	16.4	0.8
Truncation from C-terminus	OctP-cP	SDpYMNMT	16.5	0.7
	OctP-cTP	SDpYMNM	15.9	1.3
	OctP-cMTP	SDpYMN	13.6	3.6
	OctP-cNMTP	SDpYM	10.8	6.4
	OctP-cMNMTP	SDpY	9.2	8.0

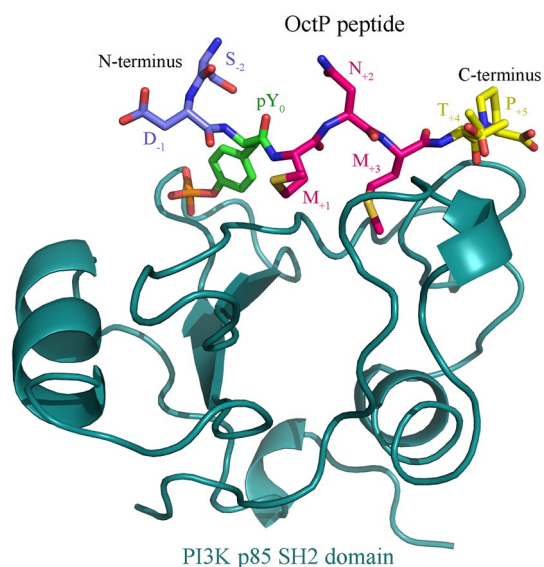[a]Score calculated via LIE approach (Gutiérrez-de-Terán and Aqvist 2012)

Fig. 3 Crystal structure of PI3K p85 SH2 domain in complex with OctP peptide (PDB: 5GJI). The two N-terminal residues S_{-2} and D_{-1} are out of the domain pocket, while the two C-terminal residues T_{+4} and P_{+5} are bound weakly to the pocket

The LIE score of native OctP peptide was estimated as 17.2, which has not significant degradation when the first two N-terminal residue S_{-2} and D_{-1} (Oct-nS and OctP-nSD, respectively) as well as the two C-terminal residues T_{+4} and P_{+5} (OctP-cP and OctP-cTP, respectively) were removed, with score values varying within a small range between 15.9 and 17.2 kcal/mol. However, a further truncation would largely reduce peptide binding capability to the domain. For example, the truncated peptides OctP-cMTP and OctP-cNMTP have only one and two-residue difference at C-terminus, but their LIE scores differ considerably to that of native OctP peptide, with ΔScore of 3.6 and 6.4, respectively. In this respect, it is suggested that the first two N-terminal residues and the two C-terminal residues should contribute modestly to OctP peptide binding, which can be removed from the peptide sequence but do not influence the peptide affinity substantially. Subsequently, the core binding motif $pY_0M_{+1}N_{+2}M_{+3}$ of OctP peptide would be used as structural scaffold to perform virtual screening of SH2 targeting compounds.

Screening, Analysis and Assay of SH2-Binding Compounds

The core binding motif pYMNM is the N- and C-truncated version of OctP peptide, which can be assigned with the indicate OctP-nSDcTP. The co-crystallized conformation of OctP-nSDcTP peptide in complex with PI3K p85 SH2 domain was stripped from the SH2–OctP complex crystal structure (PDB: 5GJI), where those domain residues

that are within 5 Å were used to define the core binding site of the domain, namely, Arg340, Arg358, Asp359, Ala360, Ser361, Thr362, Thr369, Lys379, Leu380, Ile381, Lys382, Phs392, Ser393, Leu413, Tyr416, Asb417, Lys419 and Leu420. As can be seen, the site is a mix of positively charged and hydrophobic residues, indicating a typical amphipathy. Next, >60,000 selected compounds with diverse structure, good druglikeness, and satisfactory pharmacokinetic profile were one-by-one docked into the site by using AutoDock Vina method (Trott and Olson 2010), and the docked complex structures were then subjected to OPLS all-atom force field minimization (Robertson et al. 2015). The BS between the domain and compounds was evaluated with X-Score approach (Wang et al. 2002), and the CS between the docked compounds and OctP-nSDcTP was calculated using Screen3D method (Kalászi et al. 2014). Consequently, a number of compounds with both high BS (>8.0) and large CS (>0.7) were automatically obtained, from which we manually selected eight hit compounds that are commercially available and have satisfactory structure profile as SH2 binders in a rule of thumb (Table 2).

The docked binding conformations of the eight compounds were superposed onto the co-crystallized conformation of OctP-nSDcTP peptide, shown in Fig. 4. As can be seen, the binding modes of these compounds as well as OctP-nSDcTP exhibit a good consistence, where their negatively charged moieties locate at the same site in SH2 pocket, suggesting that the selected compounds would target the domain in a similar manner with the cognate OctP-nSDcTP peptide. In this respect, the binding affinity (K_d) of the eight hit compounds, as well as OctP-nSDcTP and OctP peptides (for comparison purpose), to the recombinant protein of human PI3K p85 SH2 domain were determined by fluorescence-based assay (Table 2). As can be seen, the intact OctP peptide can bind to the domain with a high affinity ($K_d = 15$ μM); truncation of the peptide, resulting in OctP-nSDcTP, would only impair the affinity moderately ($K_d = 36$ μM), confirming that the core binding motif OctP-nSDcTP plays an essential role in OctP binding. Thus, the 3D structure-based screening of SH2-binding compounds using the OctP-nSDcTP as template is considered as an effective and feasible approach. As listed in Table 2, five out of the eight tested hit compounds exhibit moderate or high affinity towards the SH2 domain, with K_d range between 25 and 360 μM, in which two compounds, namely, hits 5 and 7, have a comparable or better binding potency relative to OctP and OctP-nSDcTP peptides ($K_d = 25$ and 37 vs. $K_d = 15$ and 32 μM), while other three compounds (hits 3, 4 and 8) can also bind moderately or weakly to the domain, with K_d values of 78, 190 and 360 μM, respectively. In addition, there are three tested compounds (i.e. hits 1, 2 and

Table 2 The eight hit compounds as well as the OctP peptide and its core OctP-*n*SD*c*TP peptide
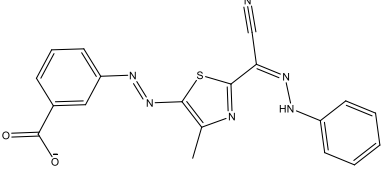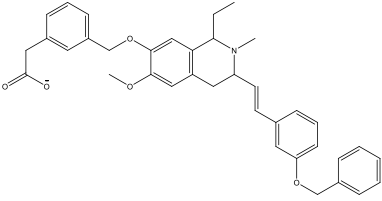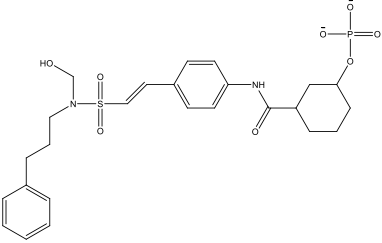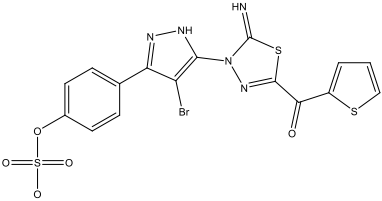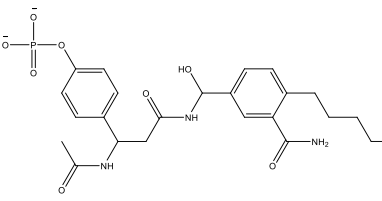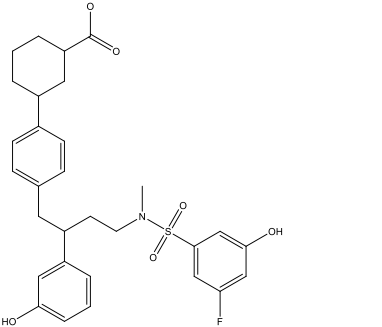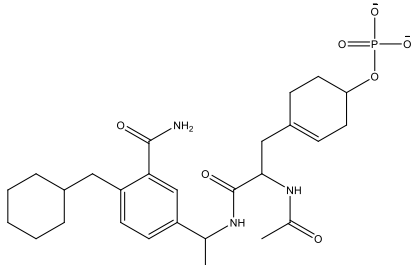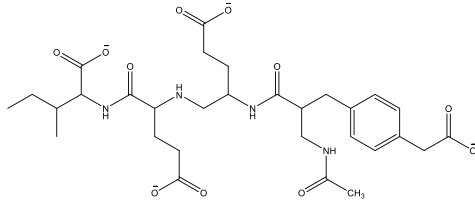
Assignment	Peptide sequence/chemical structure	BS[a]	CS[b]	K_d (µM)[c]
OctP	SDpYMNMTP	–	–	15
OctP-*n*SD*c*TP	pYMNM	–	–	32
Hit 1		8.2	0.72	n.d.
Hit 2		9.5	0.89	n.d.
Hit 3		9.1	0.82	78
Hit 4		8.1	0.74	190
Hit 5		9.8	0.84	25
Hit 6		8.7	0.76	n.d.

Table 2 (continued)

Assignment	Peptide sequence/chemical structure	BS[a]	CS[b]	K_d (µM)[c]
Hit 7		8.9	0.78	37
Hit 8		9.1	0.70	360

[a]BS: binding strength evaluated by X-Score (Wang et al. 2002)

[b]CS: conformational similarity calculated by Screen3D (Kalászi et al. 2014)

[c]K_d: experimental binding affinity measured by fluorescence-based assay
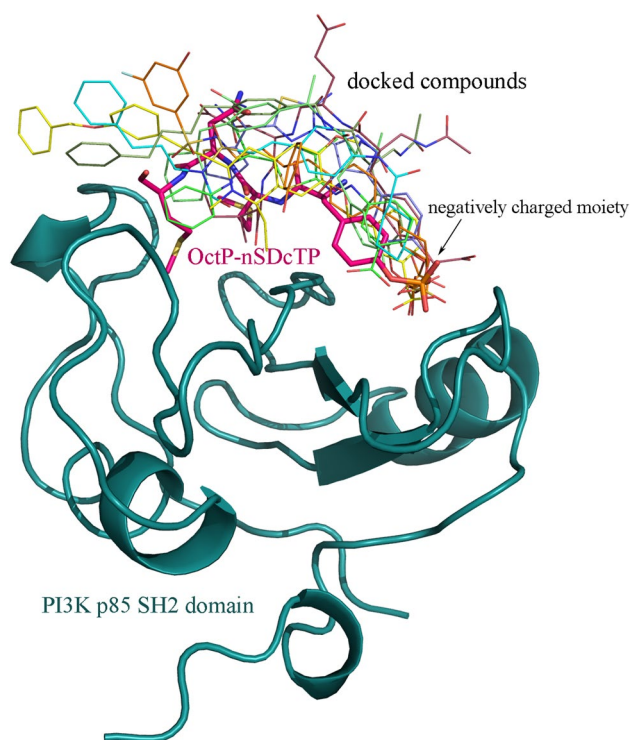

Fig. 4 Superposition of the docked binding conformations of eight hit compounds onto the co-crystallized conformation of OctP-*n*SD*c*TP peptide

6) that were determined as nonbonders of SH2 domain. By examining their chemical structures it is found that the three nonbonders share a common carboxyl group as their negatively charged anchor, which may not be compatible with the SH2 domain that is naturally designed to accommodate negatively charged phosphate moiety, although a weak binder (hit 4, $K_d = 190$ µM) possesses a sulfate in stead of the phosphate moiety.

Nonbonded interactions at the complex interfaces of SH2 domain with OctP-*n*SD*c*TP peptide ($K_d = 32$ µM) and the potent compound hit 5 ($K_d = 25$ µM) were identified by using PLIP server (Salentin et al. 2015) based on their (co-crystallized or computationally modeled) complex structures and compared in Fig. 5. It is evident that the peptide and the compound have a similar nonbonded interaction pattern with SH2 domain, that is, the negatively charged phosphate can form three electrostatic salt bridges with the basic domain residues Arg340, Arg358 and Lys382, while a number of specific hydrogen bonds and a wide hydrophobic interface can also be observed in the two complexes. The similar nonbonded pattern demonstrates that the identified compound can adopt a consistent binding mode as the template scaffold OctP-*n*SD*c*TP to interact with SH2 domain. A detailed analysis revealed that the compound hit 5 can form one more hydrogen bond and two more π–π stacking with the domain as compared to OctP-*n*SD*c*TP; thus the former can bind more tightly than the latter ($K_d = 25$ and 32 µM, respectively). In this respect, these peptide scoffed-based identified compounds could be used as lead molecular entities to further design and develop new anticancer drugs targeting the PI3K p85 SH2 domain.
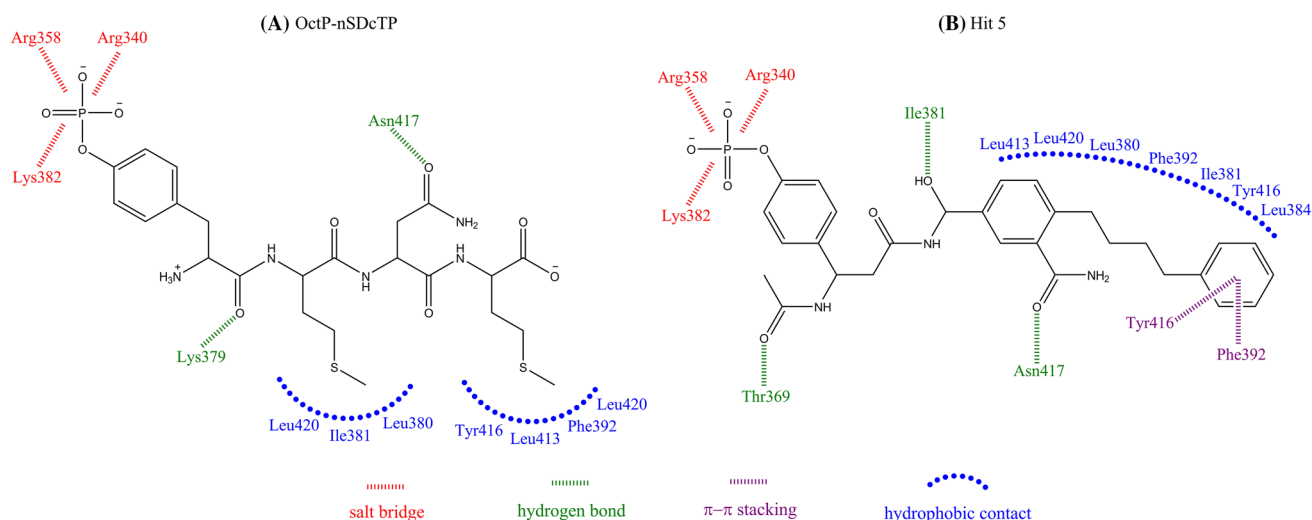
Fig. 5 Comparison of Nonbonded interactions across the complex interfaces of PI3K p85 SH2 domain with OctP-*n*SD*c*TP peptide (**a**) and potent compound hit 5 (**b**). The nonbonded interactions were identified using PLIP server (Salentin et al. 2015)

Compliance with Ethical Standards

Conflict of interest The author(s) declare that they have no conflict of interest.

References

Bai Z, Hou S, Zhang S, Li Z, Zhou P (2017) Targeting self-binding peptides as a novel strategy to regulate protein activity and function: a case study on the proto-oncogene tyrosine proteinkinase *c*-Src. J Chem Inf Model. doi:10.1021/acs.jcim.6b00673

Bas DC, Rogers DM, Jensen JH (2008) Very fast prediction and rationalization of pKa values for protein-ligand complexes. Proteins 73:765–783

Chen B, Greenside P, Paik H, Sirota M, Hadley D, Butte AJ (2015) Relating chemical structure to cellular response: an integrative analysis of gene expression, bioactivity, and structural data across 11,000 compounds. CPT Pharmacomet Syst Pharmacol 4:576–584

Chia S, Gandhi S, Joy AA, Edwards S, Gorr M, Hopkins S, Kondejewski J, Ayoub JP, Califaretti N, Rayson D, Dent SF (2015) Novel agents and associated toxicities of inhibitors of the PI3K/Akt/mtor pathway for the treatment of breast cancer. Curr Oncol 22:33–48

Dolinsky TJ, Czodrowski P, Li H, Nielsen JE, Jensen JH, Klebe G, Baker NA (2007) PDB2PQR: expanding and upgrading automated preparation of biomolecular structures for molecular simulations. Nucleic Acids Res 35:W522–W525

Enriquez-Barreto L, Morales M (2016) The PI3K signaling pathway as a pharmacological target in Autism related disorders and Schizophrenia. Mol Cell Ther 4:2

Fresno Vara JA, Casado E, de Castro J, Cejas P, Belda-Iniesta C, González-Barón M (2004) PI3K/Akt signalling pathway and cancer. Cancer Treat Rev 30:193–204

Gan W, Roux B (2009) Binding specificity of SH2 domains: insight from free energy simulations. Proteins 74:996–1007

Geuna E, Milani A, Martinello R, Aversa C, Valabrega G, Scaltriti M, Montemurro F (2015) Buparlisib, an oral pan-PI3K inhibitor for the treatment of breast cancer. Expert Opin Investig Drugs 24:421–431

Gutiérrez-de-Terán H, Aqvist J (2012) Linear interaction energy: method and applications in drug design. Methods Mol Biol 819:305–323

Inaba S, Numoto N, Ogawa S, Morii H, Ikura T, Abe R, Ito N, Oda M (2017) Crystal structures and thermodynamic analysis reveal distinct mechanisms of CD28 phosphopeptide binding to the Src homology 2 (SH2) domains of three adaptor proteins. J Biol Chem 292:1052–1060

Irwin JJ, Shoichet BK (2005) ZINC: a free database of commercially available compounds for virtual screening. J Chem Inf Model 45:177–182

Jean S, Kiger AA (2014) Classes of phosphoinositide 3-kinases at a glance. J Cell Sci 127:923–928

Kalászi A, Szisz D, Imre G, Polgár T (2014) Screen3D: a novel fully flexible high-throughput shape-similarity search method. J Chem Inf Model 54:1036–1049

Kiran MD, Adikesavan NV, Cirioni O, Giacometti A, Silvestri C, Scalise G, Ghiselli R, Saba V, Orlando F, Shoham M, Balaban N (2008) Discovery of a quorum-sensing inhibitor of drug-resistant staphylococcal infections by structure-based virtual screening. Mol Pharmacol 73:1578–1586

Liao Z, Gu L, Vergalli J, Mariani SA, De Dominici M, Lokareddy RK, Dagvadorj A, Purushottamachar P, McCue PA, Trabulsi E, Lallas CD, Gupta S, Ellsworth E, Blackmon S, Ertel A, Fortina P, Leiby B, Xia G, Rui H, Hoang DT, Gomella LG, Cingolani G, Njar V, Pattabiraman N, Calabretta B, Nevalainen MT (2015) Structure-based screen identifies a potent small molecule inhibitor of Stat5a/b with therapeutic potential for prostate cancer and chronic myeloid leukemia. Mol Cancer Ther 14:1777–1793

Lipinski CA, Lombardo F, Dominy BW, Feeney PJ (2001) Experimental and computational approaches to estimate solubility and permeability in drug discovery and development settings. Adv Drug Deliv Rev 46:3–26

Morris GM, Huey R, Lindstrom W, Sanner MF, Belew RK, Goodsell DS, Olson AJ (2009) Autodock4 and AutoDockTools4:

automated docking with selective receptor flexiblity. J Comput Chem 16:2785–2791

Pawson T, Gish GD, Nash P (2001) SH2 domains, interaction modules and cellular wiring. Trends Cell Biol 11:504–511

Robertson MJ, Tirado-Rives J, Jorgensen WL (2015) Improved peptide and protein torsional energetics with the OPLSAA force field. J Chem Theory Comput 11:3499–3509

Rodon J, Dienstmann R, Serra V, Tabernero J (2013) Development of PI3K inhibitors: lessons learned from early clinical trials. Nat Rev Clin Oncol 10:143–153

Salentin S, Schreiber S, Haupt VJ, Adasme MF, Schroeder M (2015) PLIP: fully automated protein-ligand interaction profiler. Nucleic Acids Res 43:W443–W447

Schmidt H, Hoffmann S, Tran T, Stoldt M, Stangler T, Wiesehan K, Willbold D (2007) Solution structure of a Hck SH2 domain ligand complex reveals novel interaction modes. J Mol Biol 365:1517–1532

Segall M, Champness E, Obrezanova O, Leeding C (2009) Beyond profiling: using ADMET models to guide decisions. Chem Biodivers 6:2144–2151

Thorpe LM, Yuzugullu H, Zhao JJ (2015) PI3K in cancer: divergent roles of isoforms, modes of activation and therapeutic targeting. Nat Rev Cancer 15:7–24

Trott O, Olson AJ (2010) AutoDock Vina: improving the speed and accuracy of docking with a new scoring function, efficient optimization and multithreading. J Comput Chem 31:455–461

Vuylsteke P, Huizing M, Petrakova K, Roylance R, Laing R, Chan S, Abell F, Gendreau S, Rooney I, Apt D, Zhou J, Singel S, Fehrenbacher L (2016) Pictilisib PI3Kinase inhibitor (a phosphatidylinositol 3-kinase [PI3K] inhibitor) plus paclitaxel for the treatment of hormone receptor-positive, HER2-negative, locally recurrent, or metastatic breast cancer: interim analysis of the multicentre, placebo-controlled, phase II randomised PEGGY study. Ann Oncol 27:2059–2066

Wang R, Lai L, Wang S (2002) Further development and validation of empirical scoring functions for structure-based binding affinity prediction. J Comput Aided Mol Des 16:11–26

Word JM, Lovell SC, Richardson JS, Richardson DC (1999) Asparagine and glutamine: using hydrogen atom contacts in the choice of side-chain amide orientation. J Mol Biol 285:1735–1747

Wymann MP, Pirola L (1998) Structure and function of phosphoinositide 3-kinases. Biochim Biophys Acta 1436:127–150

Yang C, Zhang S, He P, Wang C, Huang J, Zhou P (2015) Self-binding peptides: folding or binding? J Chem Inf Model 55:329–342

Yang C, Zhang S, Bai Z, Hou S, Wu D, Huang J, Zhou P (2016) A two-step binding mechanism for the self-binding peptide recognition of target domains. Mol BioSyst 12:1201–1213

Yu XD, Guo AF, Zheng GH, Yang XW (2016) Design and optimization of peptide ligands to target breast cancer-positive HER2 by grafting and truncation of MIG6 peptide. Int J Pept Res Ther 22:229–236

Zhou P, Wang C, Ren Y, Yang C, Tian F (2013) Computational peptidology: a new and promising approach to therapeutic peptide design. Curr Med Chem 20:1985–1996